Letter
Vol. 40, No. 21 / November 1 2015 / *Optics Letters* 5003

Optics Letters

# High-sensitivity distributed transverse load sensor with an elliptical-core fiber based on Brillouin dynamic gratings

Yongkang Dong,[1,*] Lei Teng,[1] Peilin Tong,[1] Taofei Jiang,[1] Hongying Zhang,[2] Tao Zhu,[3] Liang Chen,[4] Xiaoyi Bao,[4] and Zhiwei Lu[1,5]

[1]*National Key Laboratory of Science and Technology on Tunable Laser, Harbin Institute of Technology, Harbin 150001, China*
[2]*Institute of Photonics and Optical Fiber Technology, Harbin University of Science and Technology, Harbin 150080, China*
[3]*Key Laboratory of Optoelectronic Technology and Systems, Chongqing University, Chongqing 400044, China*
[4]*Fiber Optics Group, Department of Physics, University of Ottawa, Ottawa K1N 6N5, Canada*
[5]*e-mail: lvzw@hit.edu.cn*
**Corresponding author: aldendong@gmail.com*

*Received 6 August 2015; revised 25 September 2015; accepted 29 September 2015; posted 30 September 2015 (Doc. ID 247355); published 23 October 2015*

**A high-sensitivity distributed transverse load sensor based on Brillouin dynamic gratings (BDGs) is proposed and demonstrated experimentally for the first time, to the best of our knowledge. The principle is to measure the transverse-load-induced birefringence change through exciting and probing a BDG in an elliptical-core polarization-maintaining fiber. A distributed measurement of transverse load is demonstrated experimentally using a 10 m sensing fiber, which features high sensitivity to a transverse load with a measurement accuracy as high as $0.8 \times 10^{-3}$ N/mm at a 20 cm spatial resolution.** 

***OCIS codes:*** (190.4370) Nonlinear optics, fibers; (290.5900) Scattering, stimulated Brillouin; (050.2770) Gratings.

http://dx.doi.org/10.1364/OL.40.005003

In recent years, increased attention has been paid to transverse-load-sensing techniques in optical fibers [1–10] because of their applications in structural health monitoring and the civil engineering field. Optical fiber sensors based on fiber Bragg gratings (FBGs) fabricated in high-birefringence (Hi-Bi) fibers were used to measure transverse load by calculating the frequency separation of the two peaks from the slow and fast axes [2–6]. Sagnac fiber loops, including a segment of Hi-Bi fiber as the sensing element, were also used with a high sensitivity to the external transverse load by measuring the transmission interference fringes [7–9]. Moreover, some special optical fibers, such as microstructure photonic crystal fibers [4,7–9] and multicore fibers [6], have been designed to enhance the measurement sensitivity. However, point-sensing techniques, such as those developed with FBGs or Sagnac loops, cannot realize a distributed measurement. In 2010, distributed transverse load sensing with high spatial resolution (2 cm) was proposed, using an optical frequency-domain reflectometer (OFDR), which is based on recording the characteristic Rayleigh scattering spectrum of the fiber [10]. In [10], the sensitivity coefficient was measured to be 73 $\mu\varepsilon/\mathrm{Nmm}^{-1}$, and the strain measurement accuracy of the OFDR used in the experiment was a few $\mu\varepsilon$ [10], so the transverse load measurement accuracy was estimated to be $\sim 2 \times 10^{-2}$ N/mm.

Brillouin-scattering-based fiber sensors have been developed for two decades and are widely used in external physical parameter distributed sensing areas, such as temperature and strain [11]. However, traditional Brillouin distributed fiber sensing systems are insensitive to transverse load. In recent years, Brillouin dynamic gratings (BDGs) have been used in many applications, including microwave photonic filtering [12], controllable delay lines [13], distributed sensing [14–18], optical signal processing [19], light storage [20], and optical spectrum analysis [21]. It has been demonstrated experimentally that optical sensing based on BDG has a high sensitivity to the birefringence changes induced by the external parameters [14,16,18,22].

In this Letter, we propose a high-sensitivity distributed transverse load sensor based on BDG with elliptical-core (ECORE) polarization-maintaining fibers (PMFs). This distributed transverse load sensor exhibits a measurement accuracy as high as $0.8 \times 10^{-3}$ N/mm with a 20 cm spatial resolution. Since the birefringence of Panda fibers usually has a high sensitivity to temperature, there is always temperature cross talk for birefringence-based sensing. In this work, the temperature sensitivity of ECORE fiber is almost an order of magnitude lower than that of Panda fiber [14], exhibiting weaker temperature cross talk.

The BDG is optically refractive index modulated, like a fiber Bragg grating, through stimulated Brillouin scattering (SBS) [14–18,21,23,24]. As shown in Fig. 1, two counter-propagating pump waves, pump 1 and pump 2, have a frequency offset equal to the Brillouin frequency shift (BFS) of the fiber. Two pump waves are launched into the $x$ axis of the ECORE fiber to excite a BDG, and a probe wave is launched into the $y$ axis to probe the grating. A maximum probe reflection signal can be

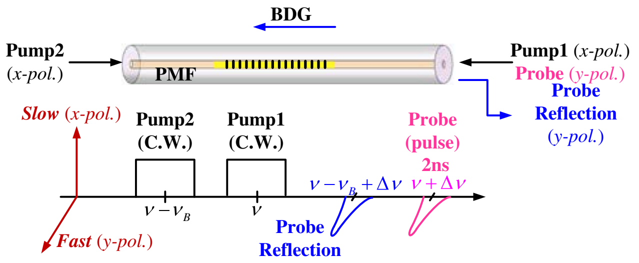


**Fig. 1.** Operational scheme of a BDG in a PMF.

obtained when the frequency difference between the probe wave and pump 1, which propagates in the same direction as the probe wave, satisfies the phase matching condition [22–24]:

$$\Delta\nu_{\mathrm{Bire}} = \Delta n / n_g \nu,$$

where $\Delta\nu_{\mathrm{Bire}}$ is the birefringence-induced frequency shift (BireFS), $\Delta n$ is the phase birefringence of the PMF, $n_g$ is the group refractive index, and $\nu$ is the frequency of the probe wave. The BDG spectrum can be obtained by recording the reflection signals while sweeping the optical frequency of the probe.

The ECORE fiber used in the experiment, as shown in inset 1 of Fig. 2, has a mode-field diameter of 13 μm × 8 μm, a nominal beat length of about 9 mm at 1310 nm (referenced from the product specification), and a measured Brillouin frequency shift of 9.894 GHz at 1550 nm at room temperature. The Brillouin gain spectrum is obtained with a line width of ~45 MHz, as measured by a traditional BOTDA system.

The experimental setup of the distributed transverse load sensor based on the BDG is depicted in Fig. 2. As shown in inset 2 of Fig. 2, the two ends of the ECORE fiber, working as the sensing fiber, are spliced with precise axial alignment to two Panda fibers by arc fusion. The output of a tunable laser at ~1550 nm with a line width of less than 100 kHz is split

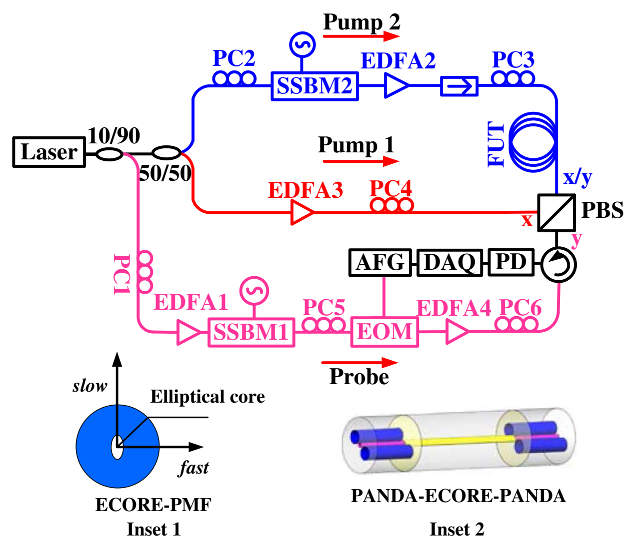


**Fig. 2.** Experimental setup of distributed transverse load sensing based on BDG. Inset 1: sectional view of ECORE fiber. Inset 2: fiber-splicing structure, Panda-ECORE-Panda. EOM, electro-optical modulator; SSBM, single-sideband modulator; PBS, polarization beam splitter; AFG, arbitrary-function generator; PD, photodiode; DAQ, data-acquisition card.

into two parts by a 10/90 coupler, where 90% is used to supply the pumps, and 10% is used as the probe light. The upper arm is divided by a 50/50 coupler, acting as the two pumps: the Brillouin pump wave (pump 1) is prepared by amplifying the original-frequency wave of the laser and is polarized to $x$ pol. by polarization controller (PC4); a single-sideband modulator (SSBM2) and a microwave synthesizer with an output frequency of 9.894 GHz are used to generate the Stokes wave (pump 2), which is polarized to $x$ pol. through a polarization beam splitter (PBS) and PC3. Modulated by another microwave synthesizer with an output frequency ranging from 14.4 to 15 GHz, SSBM1 is used to generate the probe light, which is then modulated by a high-extinction-ratio electro-optic modulator (EOM) to generate a 2 ns Gaussian pulse to read the BDG and polarized to $y$ pol. by PC6. The probe reflection wave can be received and recorded by a photodiode (PD) and data-acquisition (DAQ) card, with 1000 times averaging used in our experiment. The powers of the two pumps (pump 1 and pump 2) and the probe light are 25 dBm, 4 dBm, and 31 dBm, respectively, where a relatively low power is chosen for CW pump 2 to avoid depletion of pump 1 and, subsequently, to obtain a uniform grating over the entire fiber.

As depicted in Fig. 3, a 10 m ECORE fiber is used as the sensing fiber with a 20 cm coating-stripped segment (from 30 to 50 cm) embedded between a 20 cm glass plate and a controlled 50 cm metal support platform. The fiber coating is made up of polymer materials, such as acrylate, which act as a kind of cushioning layer, and will reduce the sensitivity of the fiber to a transverse load. A 50 cm coating-stripped single-mode fiber (SMF) is also used as the supporting fiber; since the SMF has the same structural mechanical properties as the ECORE fiber, including the geometric size, the Young's modulus, and the Poisson's ratio, when applying the load in the middle of the two fibers, each fiber carries half of the load. The sensing fiber was held under a low axial strain to prevent unwanted twist by the two rotary mounts, which were also used to control the applied loading direction relative to the ECORE fiber axes with an angular resolution of 5°.

We first investigated the temperature characteristics of the ECORE fiber from −20°C to 30°C, and the results are shown in Fig. 4, where the BireFS of the ECORE fiber has a negative temperature coefficient and the slope is −6.53 MHz/°C. Compared with the temperature coefficient of the Panda fiber (55 MHz/°C) [14], the ECORE fiber has a lower temperature coefficient and thus has weaker temperature cross talk.

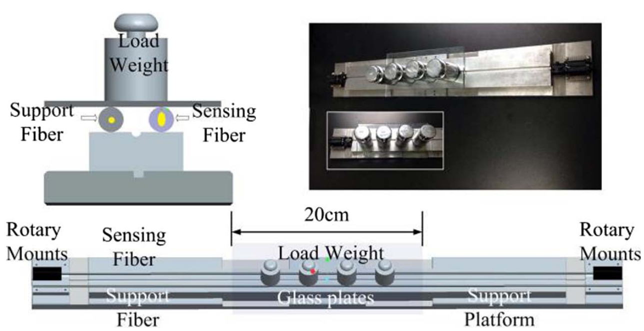


**Fig. 3.** Setup with load weight applied, utilizing two rotary mounts, two fibers (a sensing fiber and a support fiber), a 20 cm glass plate, and a 50 cm metal support platform.

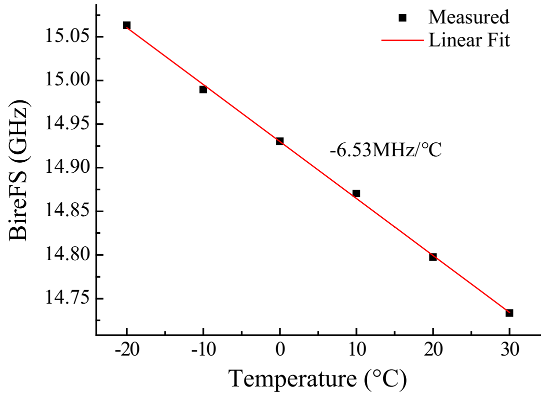


**Fig. 4.** Dependence of the BireFS of the ECORE fiber on temperature.

Figure 5 shows the change in sensitivity as a function of the orientation of the applied load when loading a weight of 5.2 N on the 20 cm glass plate, where the experimental data agree well with a sinusoidal fitting function, shown as the solid curve in Fig. 5. The maximum sensitivity occurs at ~50° (or 230°) and ~140° (or 320°), corresponding to the load direction being aligned with the slow and fast axes of the ECORE fiber, respectively, where they have a similar BireBS difference with opposite signs.

Distributed transverse load sensing with different loads and different load directions, based on BDG, has been characterized, and the results are shown in Fig. 6. When the load direction is along the fast axis, as shown in Figs. 6(a) and 6(b), the birefringence decreases with increasing load, while the birefringence increases when the load direction is along the slow axis, as shown in Figs. 6(c) and 6(d). The black curves shown in Figs. 6(a) and 6(c) are the measured results without any transverse loads, where the signal fluctuations indicate nonuniform birefringence over the fiber; this birefringence nonuniformity was also observed in other types of PMFs [18,22]. By subtracting the initial frequency shift, the BireFS difference, i.e., transverse-load-induced frequency shift, can be measured, as shown in Figs. 6(b) and 6(d). The fitting results of the distributed transverse load measurements are presented in Figs. 6(a) and 6(c) under different loads, ranging from 0 to $2.8 \times 10^{-2}$ N/mm; Figs. 6(b) and 6(d) depict the BireFS differences corresponding to Figs. 6(a) and 6(c).

Figure 7 shows the dependence of the BireFS difference on the transverse load of the ECORE fiber in both the slow-axis

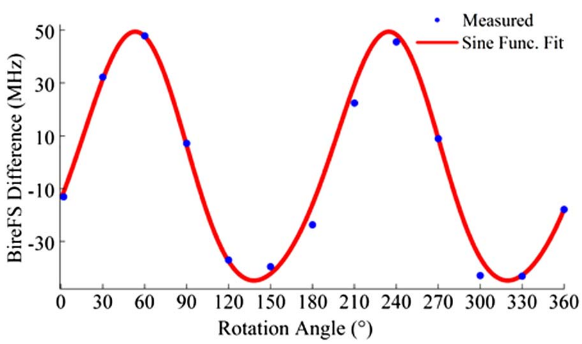


**Fig. 5.** Change in sensitivity as a function of load direction on a 20 cm long glass plate under a load weight of 5.2 N.

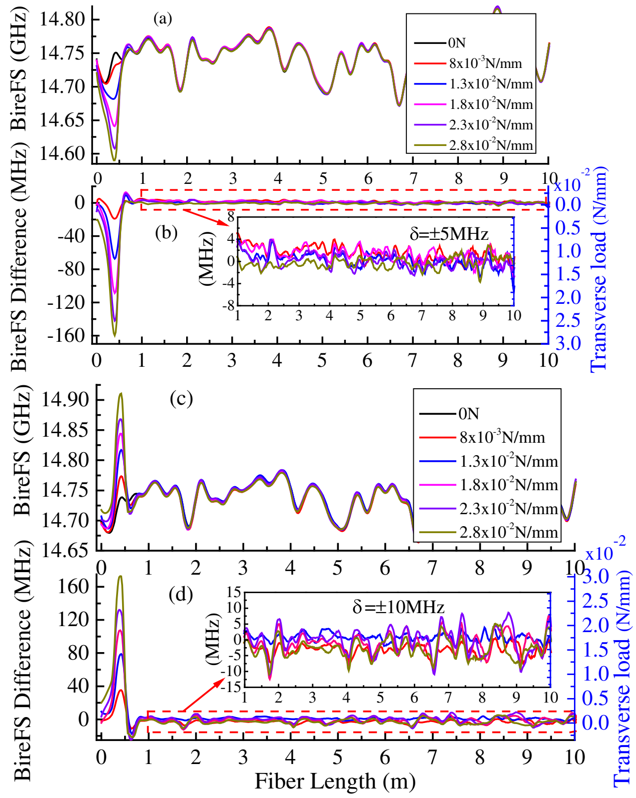


**Fig. 6.** Fitting results of distributed measurements. (a) and (c) show the distributed BireFS of the sensing fiber under different loading conditions in the fast-axis direction and the slow-axis direction, respectively; (b) and (d) show the BireFS differences corresponding to (a) and (c), respectively. Two insets show the BireFS variations for the no-transverse-load region from 1 to 10 m.

and fast-axis directions, where the experimental results illustrate the transverse load sensitivities of –6.217 $\mathrm{GHz/Nmm^{-1}}$ for the fast-axis direction and 6.28 $\mathrm{GHz/Nmm^{-1}}$ for the slow-axis direction. In Fig. 6, the fiber section from 1 to 10 m corresponds to a no-transverse-load region, so we use the variation of the BireFS difference in this region to characterize the measurement accuracy. For the transverse load direction aligned to the fast axis, as shown in the inset of Fig. 6(b), the variation is $\delta = \pm 5$ MHz, corresponding to an accuracy of $0.8 \times 10^{-3}$ N/mm, while for the slow axis, as shown in the inset of Fig. 6(d), the variation is $\delta = \pm 10$ MHz, corresponding to an accuracy of $1.6 \times 10^{-3}$ N/mm. Since the ECORE fiber and the Panda fiber have different mode-field areas, different (slight) polarization cross talk may be introduced for an individual splicing, which contributes to the difference in measurement accuracy for the two cases.

In addition, in order to verify the distributed measurement and the direction-sensitive feature of transverse load sensing, simultaneous measurements of two transverse loads applied on two 20 cm stripped parts of the sensing fiber were performed with $2.3 \times 10^{-2}$ N/mm applied loads in the two orthogonal directions—a load along the fast axis and the slow axis, respectively. The distributed measurement results are shown in Fig. 8, which shows a comparison of measured BireFS under the conditions with and without loads in two parts; Fig. 8(b) shows the BireFS difference after applying load, which clearly indicates the magnitude and the direction of the load.

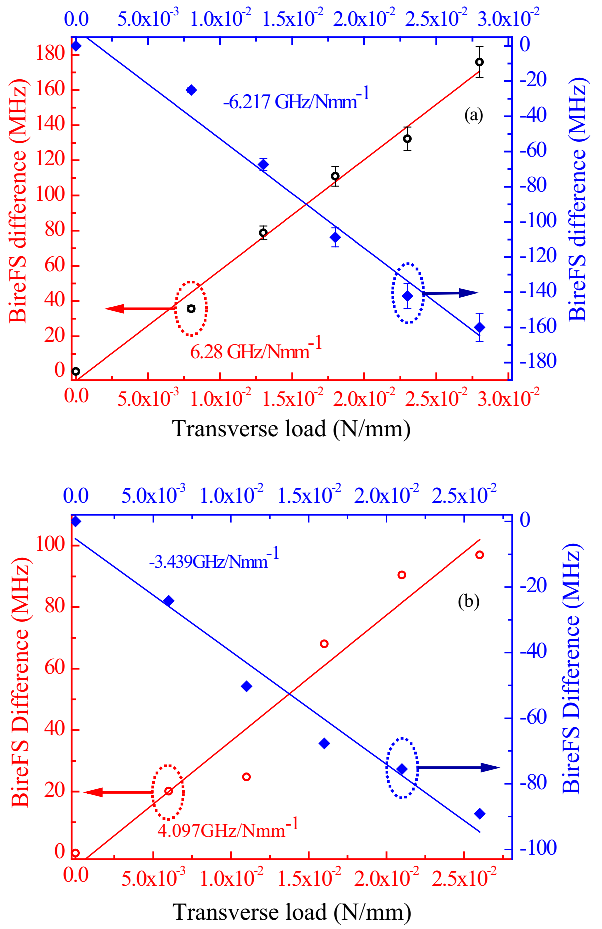


**Fig. 7.** BireFS differences versus transverse loads ranging from 0 to $2.8 \times 10^{-2}$ N/mm in the slow-axis direction (red) and the fast-axis direction (blue) for (a) ECORE fiber and (b) Panda fiber.

We also measured the transverse load sensitivities of the Panda fiber shown in Fig. 7(b), which are measured to be 4.097 and −3.439 GHz/Nmm$^{-1}$ for the slow and fast axes; they are slightly smaller than those of the ECORE fiber. Because the Panda fiber has a large BireFS of ~55.3 GHz, a free-running tunable laser was used as the probe wave, resulting in a relatively large measurement error, which can be reduced by locking the frequency offset between the pump and probe waves. It is believed that the high sensitivity of this method is mainly due to the high-accuracy measurement of the BDG spectrum.

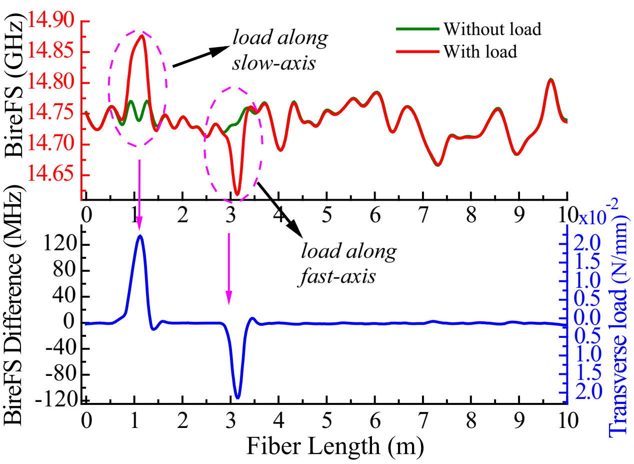


**Fig. 8.** Distributed transverse load measurements of two 20 cm segments with applied perpendicular loads of $2.3 \times 10^{-2}$ N/mm: (a) the measured BireFS with and without loads and (b) the BireFS difference after applying loads.

To summarize, we have proposed and experimentally demonstrated a high-sensitivity distributed transverse load sensor based on BDG. The experimental setup adopted two continuous waves to excite a BDG and a short probe pulse (2 ns) to map the Brillouin grating spectrum associated with the birefringence in an elliptical-core polarization maintaining fiber with a spatial resolution of 20 cm. The sensing technique features a distributed measurement, directional sensitivity, and a high sensitivity to transverse load, with a measurement accuracy as high as $0.8 \times 10^{-3}$ N/mm at a 20 cm spatial resolution. In addition, the ECORE fiber has a lower temperature cross talk compared to the Panda fiber.

**Funding.** 863 Program of China (2014AA110401); National Key Scientific Instrument and Equipment Development Project of China (2013YQ040815); National Key Technology Research and Development Program of the Ministry of Science and Technology of China (2014BAG05B07); National Natural Science Foundation of China (NSFC) (61205073, 61308004); Scientific Research Fund of Heilongjiang Provincial Education Department of China (2531093); Foundation for Talents Returning from Overseas of Harbin of China (2013RFLXJ013).

## REFERENCES

1. L. Y. Shao, Q. Jiang, and J. Albert, Appl. Opt. **49**, 35 (2010).
2. J. T. Kringlebotn, W. H. Loh, and R. I. Laming, Opt. Lett. **21**, 1869 (1996).
3. E. Chehura, C. C. Ye, and S. E. Staines, Smart Mater. Struct. **13**, 888 (2004).
4. C. Jewart, K. P. Chen, and B. McMillen, Opt. Lett. **31**, 2260 (2006).
5. Y. Zhang, T. Sun, and L. Y. Xiong, "Distributed transverse load sensing with tilted fiber Bragg gratings using optical frequency domain reflectometry," in *22nd International Conference on Optical Fiber Sensors*, Beijing, China, 2012, paper 84214S.
6. M. Silva-López, W. N. MacPherson, and C. Li, Appl. Opt. **44**, 32 (2005).
7. P. Zu, C. C. Chan, and Y. Jin, Meas. Sci. Technol. **22**, 025204 (2011).
8. C. Fan, C. Chiang, and C. Yu, Opt. Express **19**, 21 (2011).
9. Y. Yang, J. Li, and W. Duan, Meas. Sci. Technol. **24**, 9 (2013).
10. R. R. J. Maier, W. N. MacPherson, and J. S. Barton, Meas. Sci. Technol. **21**, 094019 (2010).
11. X. Bao and L. Chen, Sensors **11**, 4152 (2011).
12. J. Sancho, N. Primerov, and S. Chin, Opt. Express **20**, 6 (2012).
13. S. Chin and L. Thévenaz, Laser Photon. Rev. **6**, 724 (2012).
14. W. Zou, Z. He, and K. Hotate, Opt. Express **17**, 3 (2009).
15. K. Y. Song, S. Chin, N. Primerov, and L. Thevenaz, J. Lightwave Technol. **28**, 2818 (2010).
16. K. Y. Song and H. J. Yoon, Opt. Lett. **35**, 1 (2010).
17. K. Y. Song, Opt. Express **20**, 25 (2012).
18. Y. Dong, X. Bao, and L. Chen, Opt. Lett. **34**, 17 (2009).
19. M. Santagiustina, S. Chin, N. Primerov, L. Ursini, and L. Thévenaz, Sci. Rep. **3**, 1594 (2013).
20. H. G. Winful, Opt. Express **21**, 8 (2013).
21. Y. Dong, T. Jiang, and L. Teng, Opt. Lett. **39**, 10 (2014).
22. Y. Dong, L. Chen, and X. Bao, Opt. Lett. **35**, 2 (2010).
23. K. Y. Song, W. Zou, and Z. He, Opt. Lett. **33**, 9 (2008).
24. K. Y. Song, W. Zou, and Z. He, Opt. Lett. **34**, 2 (2009).